Title: Boson stars through the prism of numerical relativity

Speakers: Tamara Evstafyeva

Series: Strong Gravity

Date: January 25, 2024 - 1:00 PM

URL: https://pirsa.org/24010094

Abstract: The existence of fermionic compact objects, such as neutron stars, is supported by a plethora of observational evidence -- an intriguing idea is whether one can construct stars made up of the bosonic counterparts. Such theoretical objects are called boson stars, proposed to make up a fraction of the dark matter in our Universe and claimed to be promising horizonless black hole mimickers. In this talk I will discuss the state-of-the-art of numerical evolutions of boson star models in spherical symmetry. In particular, I will discuss how improper initial data construction can lead to spurious physical effects in the evolution of boson star mergers and introduce methods, necessary to remedy such spurious features. I will present our results on boson star head-on collisions of various mass ratios, highlighting the differences from the black hole mergers. Lastly, I will discuss our recent results on the high-precision numerical relativity simulations of quasi-circular boson star inspirals in pursuit of understanding the implications of boson star signatures on the LIGO-Virgo-KAGRA observations.

Zoom link

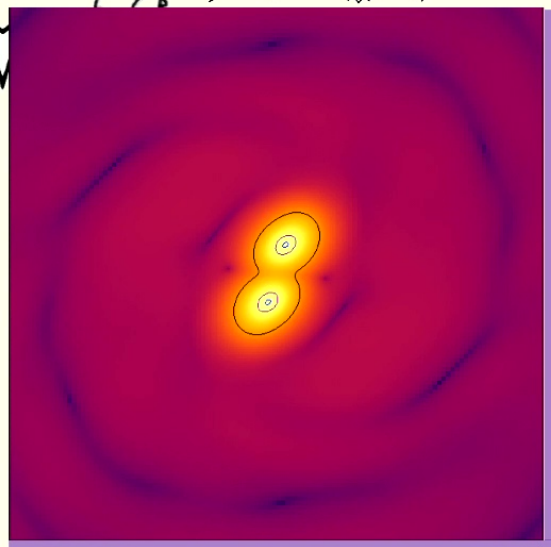
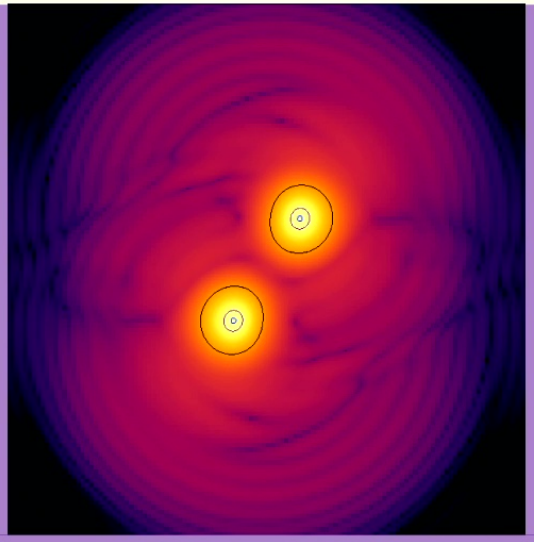
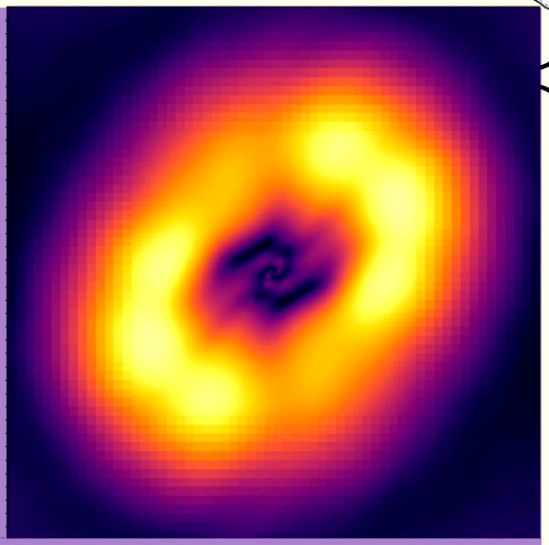

“BOSON STARS THROUGH THE PRISM OF NUMERICAL RELATIVITY”

TAMARA EVSTAFYEVA, UNIVERSITY OF CAMBRIDGE

Special thank you to my supervisor **Ulrich Sperhake**, and my collaborators: **Eugene Lim**, **Roxana Rosca-Mead**, **Thomas Helfer**, **Robin Croft**, **Miren Radia**, **Bo-Xuan Ge**, **Isobel Romero-Shaw**

Outline of this talk

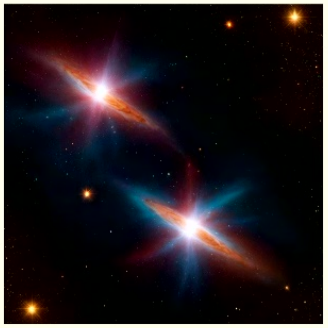

Binary boson star merger according to AI image generator

LIGO's response

Inspiralling systems

Head-on collisions

NR + initial data

Overview of boson stars and their formulation

LIGO Livingston GW detector

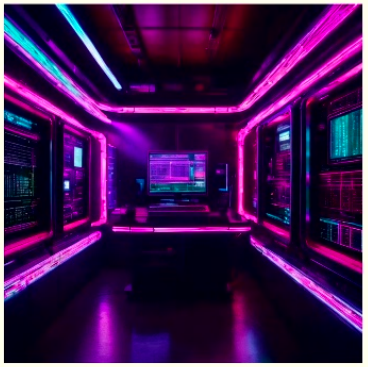

Numerical relativity according to AI image generator

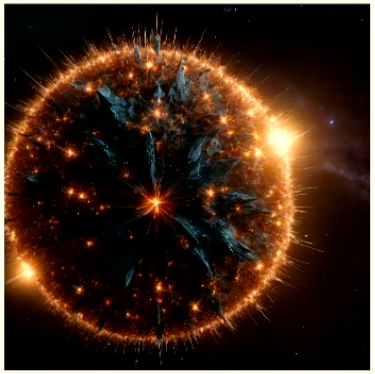

A boson star according to AI image generator

The ‘big’ picture and historical perspective

- Wheeler’s idea (1955): **gravitational electromagnetic entities** (called geons) -> found to be unstable.
- Kaup’s idea (1968): **replace electromagnetic field with a complex scalar field** -> found gravitationally bound spherically symmetric configurations of complex scalar field – boson stars (BSs)!
- Boson stars have been suggested as dark matter candidates and even alternatives supermassive BHs in the centres of galaxies. Torres (2000)
- Boson stars can form due to gravitational condensation from isotropic initial conditions.

Klein-Gordon Geon*

DAVID J. KAUP†
University of Maryland, College Park, Maryland
(Received 4 March 1968)

A study of the spherically symmetric eigenstates of the Klein-Gordon Einstein equations (Klein-Gordon geons) reveals that these geons have properties that are uniquely different from other gravitating systems that have been studied. The equilibrium states of these geons seem analogous to other gravitating systems; but when the question of stability is considered from a thermodynamical viewpoint, it is shown that, in contrast with other systems, adiabatic perturbations are forbidden. The reason is that the equations of state for the thermodynamical variables are not algebraic equations, but instead are differential equations. Consequently, the usual concept of an equation of state breaks down when Klein-Gordon geons are considered. When the question of stability is reconsidered in terms of infinitesimal perturbations of the basic fields, it is then found that Klein-Gordon geons will not undergo spherically symmetric gravitational collapse. Thus, Klein-Gordon geons are counterexamples to the conjecture that gravitational collapse is inevitable.

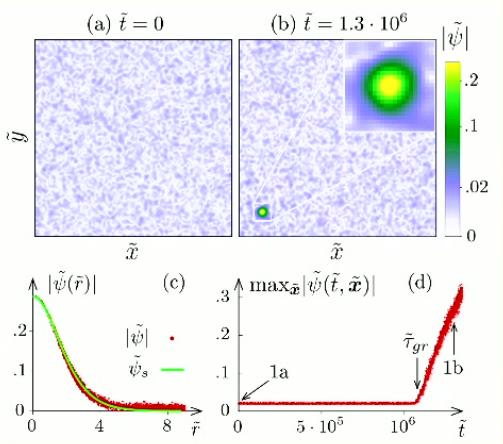

Levkov 2018

Boson stars in a nutshell

- Comprised of bosons, $\mu \in [10^{-22}, 10^{-3}] eV$, (possibly ultralight).
- Described by some **fundamental complex scalar field with potential**.
- Conserved $U(1)$ charge, Q (*Noether charge*), denoting the number of boson particles in the system and precluding the gravitational decay.
- Tendency of a localised wave solution to disperse is balanced by the gravitational attraction.
- BS mass can be in the range of $[1, 10^{10}] M_{\odot}$.

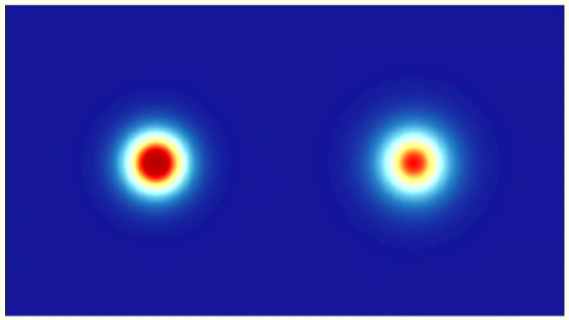

Can have light rings -> **BH mimickers**!

Have **maximum mass** (feature of most stellar structures), regulated by the mass of the fundamental boson and self-interaction terms.

BUT!

1. No horizon.
2. No surface – the scalar field extends to infinity but falls off exponentially.

Tamara's list for why study boson stars

- Increased interest in modified theories of gravity and theories beyond the Standard Model of particle physics, trying to tackle questions about the nature of dark matter, dark energy and unify GR with the quantum world.
- Increased interest in exotic compact objects: ordinary matter cannot support the enormous self-gravity of a massive and ultracompact object, so the latter is usually a BH – can it be something else?
- Neutron stars, with compactness $\sim 1/3$ cannot sustain masses larger than $\sim 3M_{\odot}$, whereas giant stars with masses $M \geq 10M_{\odot}$have compactnesses orders of magnitude smaller.

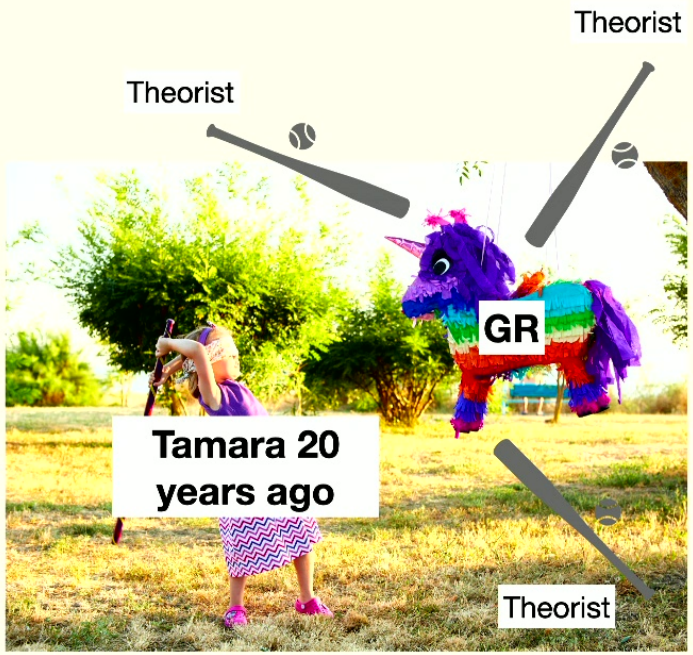

Numerical relativity and boson stars

A zoo of boson stars studied numerically

Stars made of: **spin-0 field** (boson stars, oscillatons), **spin-1 field** (Proca stars), **high-spin field**.

Kaup (1968), Colpi (1986), Lee (1987) Brito (2017) Jain & Amin (2021)

Jetzer, (1989)

Charged

l-boson stars (multiple fields)

Alcubierre, (2018)

Rotating, BSs have quantised angular momentum, $J = mQ$

Schunck & Mielke, (2018), Siemonsen, (2020)

Collodel, (2022)

Thin-shell BSs

Multi-oscillating BSs

Choptuik, (2019)

BSs with various potentials: mini, solitonic, repulsive and many more!

GRChombo – adaptive mesh refinement numerical relativity code

CCZ4 formulation (includes constraint damping terms)

4th order spatial differencing with a 4th order Runge-Kutta integration in time

Moving puncture gauge

Mathematical formulation

- **GR + minimally coupled complex scalar field φ**

$$S = \int \sqrt{-g}\left[\frac{1}{16\pi G}R - \frac{1}{2}\left(g^{\mu\nu}\nabla_\mu\varphi^*\nabla_\nu\varphi + V(\varphi)\right)\right]d^4x \qquad T_{\alpha\beta} = \partial_{(\alpha}\varphi^*\partial_{\beta)}\varphi - \frac{1}{2}g_{\alpha\beta}\left[g^{\mu\nu}\partial_\mu\varphi^*\partial_\nu\varphi + V(\varphi)\right]$$

- $V(\varphi)$ is the **scalar potential** describing the BS model (analogous to EOS):

$$V_{\mathrm{sol}} = \mu^2|\varphi|^2\left(1 - 2\frac{|\varphi|^2}{\sigma_0^2}\right)^2$$

σ_0 **quantifies the field's self-interaction**
μ **— mass of the scalar field**

$$G_{\alpha\beta} = 8\pi G T_{\alpha\beta}$$

$$\nabla^\mu\nabla_\mu\varphi = \varphi\frac{\mathrm{d}V}{\mathrm{d}|\varphi|^2}$$

Spherically symmetric solutions

- Regular solutions exist for countably infinite number of frequencies ω, via $\omega_0 < \omega_1 < \ldots < \omega_n$ relation.
- $n = 0$ – **ground states**, $n > 0$ – **excited states**. This n corresponds to the number of zero crossings of the amplitude function $A(r)$.
- **Excited states are unstable**: collapse to a BH, disperse, migrate to ground state. Balakrishna, Seidel, Suen (1998)

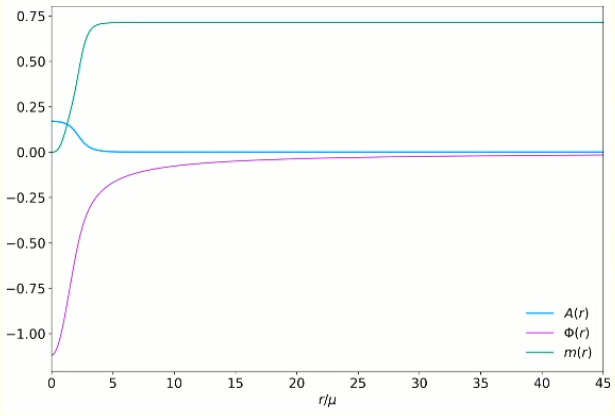

$$\varphi(t, r) = A(r)e^{i(\epsilon\omega t + \delta\phi)}$$

A - **amplitude,**
ω - **frequency,**
$\delta\phi$ - **dephasing parameter,**
$\epsilon = \pm 1$ - **boson/antiboson.**

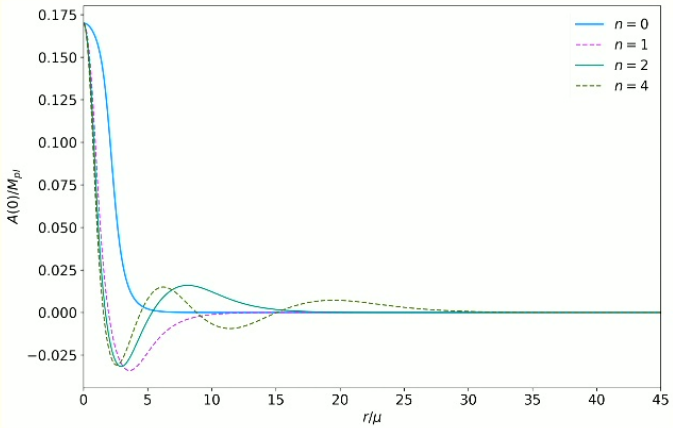

$$ds^2 = -e^{2\Phi}\mathrm{d}t^2 + \left(1 - \frac{2m}{r}\right)^{-1}\mathrm{d}r^2 + r^2\left(\mathrm{d}\theta^2 + \sin^2\theta\mathrm{d}\phi^2\right)$$

Families of solutions

- By varying $A(0)$, we can construct **families of BS solutions** for a given potential function (e.g. $\sigma_0 = 0.2$). A common feature of $M(R)$ plots is the maximum mass; for a solitonic potential this maximum mass depends on the self-interaction, σ_0.

- We define compactness measure, $C := max(m(r)/r)$.

For comparison:

$C_{NS} \sim 0.1$

$C \approx 0.22$

$C \approx 0.17$

$C \approx 0.12$

$C \approx 0.07$

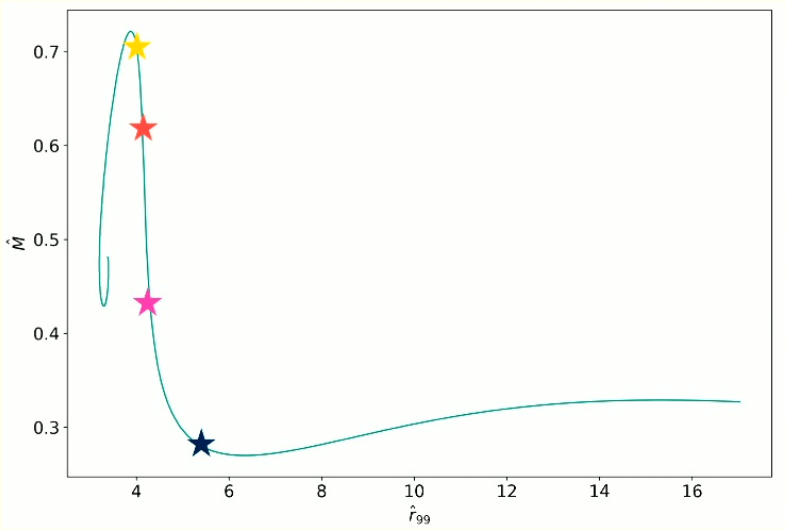

Mathematical formulation

- **GR + minimally coupled complex scalar field φ**

$$S = \int \sqrt{-g}\left[\frac{1}{16\pi G}R - \frac{1}{2}\left(g^{\mu\nu}\nabla_\mu\varphi^*\nabla_\nu\varphi + V(\varphi)\right)\right]d^4x \qquad T_{\alpha\beta} = \partial_{(\alpha}\varphi^*\partial_{\beta)}\varphi - \frac{1}{2}g_{\alpha\beta}\left[g^{\mu\nu}\partial_\mu\varphi^*\partial_\nu\varphi + V(\varphi)\right]$$

- $V(\varphi)$ is the **scalar potential** describing the BS model (analogous to EOS):

$$V_{\mathrm{sol}} = \mu^2|\varphi|^2\left(1 - 2\frac{|\varphi|^2}{\sigma_0^2}\right)^2$$

σ_0 **quantifies the field's self-interaction**
μ **— mass of the scalar field**

$$G_{\alpha\beta} = 8\pi G T_{\alpha\beta}$$

$$\nabla^\mu\nabla_\mu\varphi = \varphi\frac{\mathrm{d}V}{\mathrm{d}|\varphi|^2}$$

Spherically symmetric solutions

- Regular solutions exist for countably infinite number of frequencies ω, via $\omega_0 < \omega_1 < \ldots < \omega_n$ relation.
- $n = 0$ – **ground states**, $n > 0$ – **excited states**. This n corresponds to the number of zero crossings of the amplitude function $A(r)$.
- **Excited states are unstable**: collapse to a BH, disperse, migrate to ground state. Balakrishna, Seidel, Suen (1998)

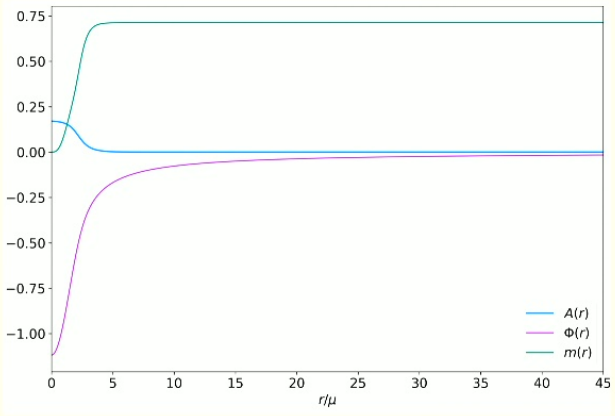

$$\varphi(t, r) = A(r)e^{i(\epsilon\omega t + \delta\phi)}$$

A - **amplitude,**
ω - **frequency,**
$\delta\phi$ - **dephasing parameter,**
$\epsilon = \pm 1$ - **boson/antiboson.**

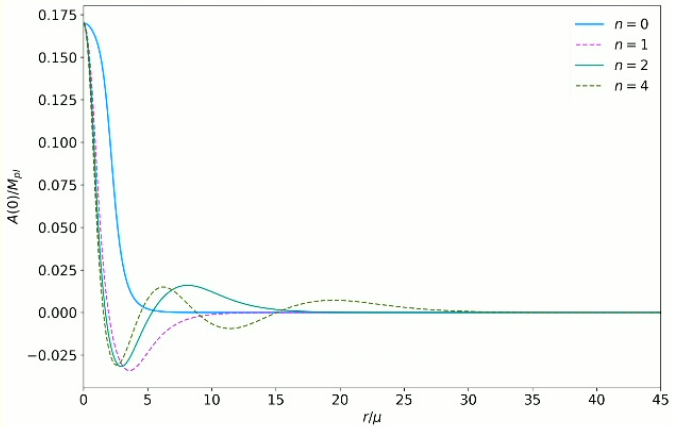

$$ds^2 = -e^{2\Phi}\mathrm{d}t^2 + \left(1 - \frac{2m}{r}\right)^{-1}\mathrm{d}r^2 + r^2\left(\mathrm{d}\theta^2 + \sin^2\theta\mathrm{d}\phi^2\right)$$

Families of solutions

- By varying $A(0)$, we can construct **families of BS solutions** for a given potential function (e.g. $\sigma_0 = 0.2$). A common feature of $M(R)$ plots is the maximum mass; for a solitonic potential this maximum mass depends on the self-interaction, σ_0.

- We define compactness measure, $C := max(m(r)/r)$.

For comparison:

$C_{NS} \sim 0.1$

$C \approx 0.22$

$C \approx 0.17$

$C \approx 0.12$

$C \approx 0.07$

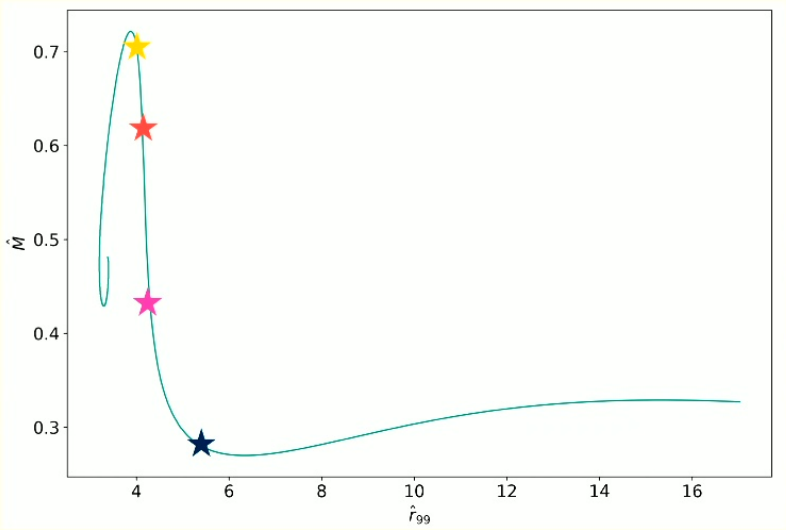

Families of solutions

- By varying $A(0)$, we can construct **families of BS solutions** for a given potential function (e.g. $\sigma_0 = 0.2$). A common feature of $M(R)$ plots is the maximum mass; for a solitonic potential this maximum mass depends on the self-interaction, σ_0.

- We define compactness measure, $C := max(m(r)/r)$.

Possible not only in GR: families of BS solutions have additional branches in the $M(R)$ plots in scalar-tensor theories of gravity. Evstafyeva, (2023)

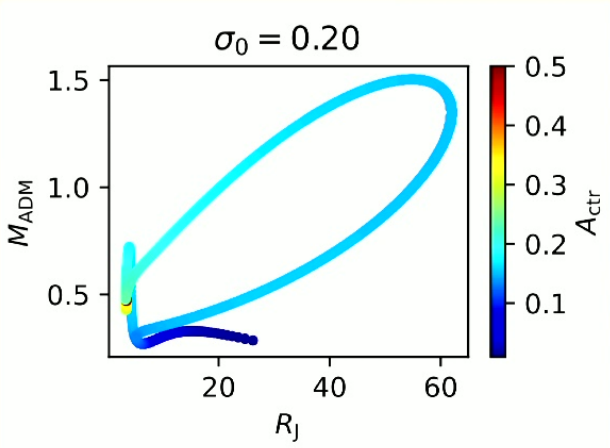

Numerical relativity and initial data

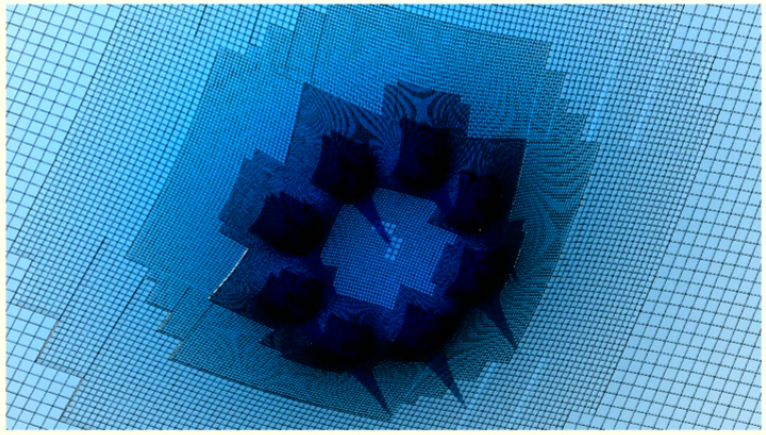

Credits: Katy Clough

Key ingredients of NR

- The spacetime metric is decomposed into spatial metric γ_{ij}, the shift vector β^i and the lapse function α:

$$ds^2 = -\alpha^2 dt^2 + \gamma_{mn}(dx^m + \beta^m dt)(dx^n + \beta^n dt)$$

- Additionally, we define an **extrinsic curvature** and **the conjugate momentum** of the scalar field:

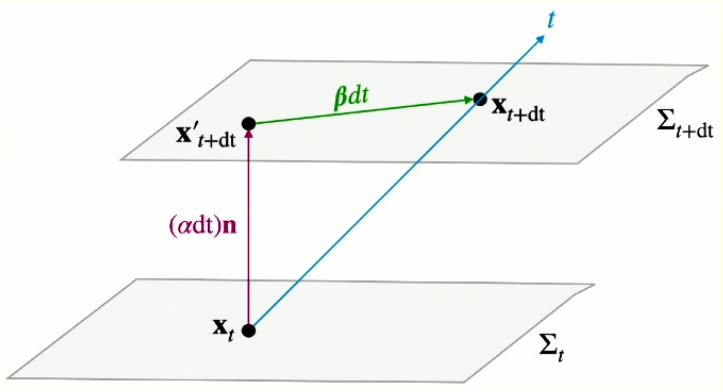

$$K_{\alpha\beta} = -(\delta^{\mu}_{\beta} + n^{\mu} n_{\beta}) \nabla_{\mu} n_{\alpha}$$

$$\Pi = -\frac{1}{2\alpha}(\partial_t \varphi - \beta^m \partial_m \varphi)$$

$$\tilde{\gamma}_{ij} = \chi \gamma_{ij}, \quad \chi = \gamma^{-1/3}, \quad \tilde{\gamma} = 1$$

$\tilde{\gamma}_{ij}$ – conformally rescaled metric

Breakdown of the equations

A bunch of **evolution equations** for the metric + scalar field sector.

$$\partial_t \chi = \beta^m \partial_m \chi + \frac{2}{3}\chi(\alpha K - \partial_m \beta^m), \tag{8}$$

$$\partial_t \tilde{\gamma}_{ij} = \beta^m \partial_m \tilde{\gamma}_{ij} + 2\tilde{\gamma}_{m(i}\partial_{j)}\beta^m - \frac{2}{3}\tilde{\gamma}_{ij}\partial_m \beta^m - 2\alpha \tilde{A}_{ij}, \tag{9}$$

$$\partial_t K = \beta^m \partial_m K - \chi \tilde{\gamma}^{mn} D_m D_n \alpha + \alpha \tilde{A}^{mn}\tilde{A}_{mn} + \frac{1}{3}\alpha K^2 + 4\pi G \alpha (S + \rho), \tag{10}$$

$$\partial_t \tilde{A}_{ij} = \beta^m \partial_m \tilde{A}_{ij} + 2\tilde{A}_{m(i}\partial_{j)}\beta^m - \frac{2}{3}\tilde{A}_{ij}\partial_m \beta^m + \alpha K \tilde{A}_{ij} - 2\alpha \tilde{A}_{im}\tilde{A}^m{}_j + \chi\{\alpha \mathcal{R}_{ij} - D_i D_j \alpha - 8\pi G \alpha S_{ij}\}^{\mathrm{TF}}, \tag{11}$$

$$\partial_t \tilde{\Gamma}^i = \beta^m \partial_m \tilde{\Gamma}^i + \frac{2}{3}\tilde{\Gamma}^i \partial_m \beta^m - \tilde{\Gamma}^m \partial_m \beta^i + \tilde{\gamma}^{mn}\partial_m \partial_n \beta^i + \frac{1}{3}\tilde{\gamma}^{im}\partial_m \partial_n \beta^n - \tilde{A}^{im}\left(3\alpha \frac{\partial_m \chi}{\chi} + 2\partial_m \alpha\right) + 2\alpha \tilde{\Gamma}^i_{mn}\tilde{A}^{mn} - \frac{4}{3}\alpha \tilde{\gamma}^{im}\partial_m K - 16\pi G \frac{\alpha}{\chi} j^i, \tag{12}$$

$$\partial_t \varphi = \beta^m \partial_m \varphi - 2\alpha \Pi,$$

$$\partial_t \Pi = \beta^m \partial_m \Pi + \alpha\left[\Pi K + \frac{1}{2}V'\varphi + \frac{1}{4}\tilde{\gamma}^{mn}\left(\partial_m \varphi \partial_n \chi - 2\chi \tilde{D}_m \tilde{D}_n \varphi\right)\right] - \frac{1}{2}\chi \tilde{\gamma}^{mn}\partial_m \varphi \partial_n \alpha$$

Constraint equations:

$$\mathscr{H} = \mathscr{R} + K^2 - K^{mn}K_{mn} - 16\pi\rho = 0$$

$$\mathscr{M}_i = D_i K - D_m K_i^m + 8\pi j_i = 0$$

Here:

$\rho = 2\Pi\bar{\Pi} + \frac{1}{2}\partial^m \bar{\varphi}\,\partial_m \varphi + \frac{1}{2}V$ is the *energy density*

$j_i = \bar{\Pi}\partial_i \varphi + \Pi \partial_i \bar{\varphi}$ is the *momentum density*

How do we satisfy the constraint equations?

Initial data: plain superposition

$$\gamma_{ij} = \gamma^{\rm A}_{ij} + \gamma^{\rm B}_{ij} - \delta_{ij}$$

$$\varphi = \varphi_{\rm A} + \varphi_{\rm B}$$

$$\Pi = \Pi_{\rm A} + \Pi_{\rm B}$$

$$K_{ij} = \gamma_{m(i}\left[K^{\rm A}_{j)n}\gamma^{mn}_{\rm A} + K^{\rm B}_{j)n}\gamma^{nm}_{\rm B}\right]$$

Spurious oscillations in the BS central amplitude.

Pre-mature BH formation (i.e. a BH forms pre-merger).

Constraint violations can be large!

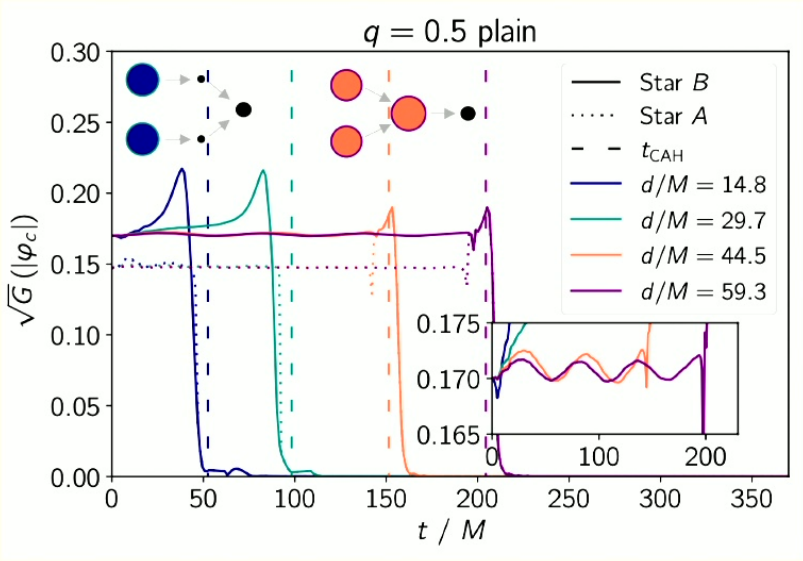

- *Why the superposition does not work as expected?*

At the centres of the stars, **plain superposition induces large deviations from the equilibrium values of the volume element,** $\sqrt{\det(\gamma_{ij})}$ Helfer+ (2019), Helfer + (2022)

Steps towards better initial data

- **Need to account for the influence of one star onto the other** – recover equilibrium volume elements at the stars' centres (only applicable for equal-mass): Helfer, (2019)

$$\gamma_{ij} = \gamma^{\mathrm{A}}_{ij} + \gamma^{\mathrm{B}}_{ij} - \gamma^{\mathrm{B}}_{ij}(x^i_{\mathrm{A}}) = \gamma^{\mathrm{A}}_{ij} + \gamma^{\mathrm{B}}_{ij} - \gamma^{\mathrm{A}}_{ij}(x^i_{\mathrm{B}}) \qquad (1)$$

- Generalised ansatz (1) to unequal-mass binaries by re-defining a conformal factor: Evstafyeva, (2023)

$$\lambda_{\mathrm{new}} = \lambda(x^i) + w_A(x^i)h_A + w_B(x^i)h_B,$$

$h_A, h_b = const.\,, w_A, w_B$ – weight functions

$$\gamma_{ij} = \gamma^{\mathrm{A}}_{ij} + \gamma^{\mathrm{B}}_{ij} - \delta_{ij},$$

$$\lambda = \gamma^{1/3}$$

Improved initial data superposition

- Significant progress made on initial data solvers for BS binaries. Siemonsen, (2023)
- Using improved initial data superpositions for equal-mass binaries produces compatible waveforms with initial data obtained from CTS solver, showing a maximum of ~2% difference. Atteneder, (2023)

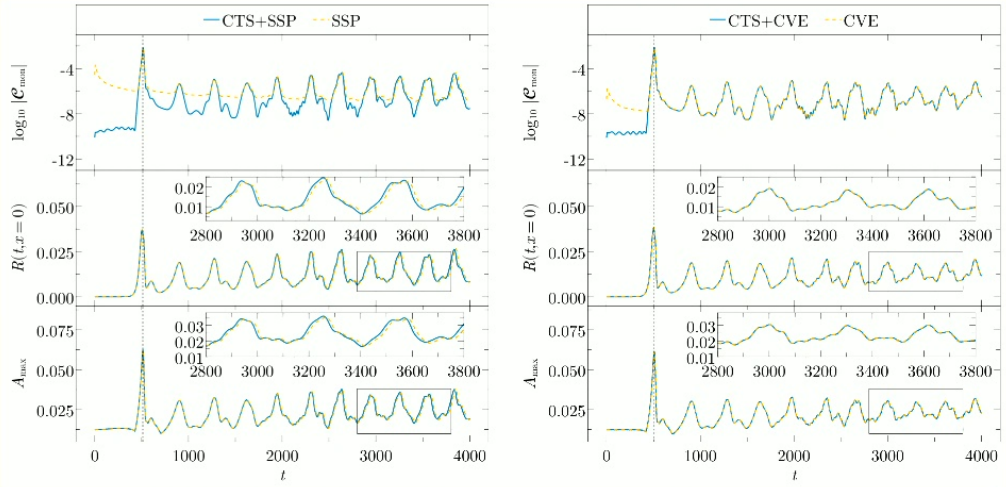

Steps towards better initial data

- **Need to account for the influence of one star onto the other** – recover equilibrium volume elements at the stars' centres (only applicable for equal-mass): Helfer, (2019)

$$\gamma_{ij} = \gamma^{\mathrm{A}}_{ij} + \gamma^{\mathrm{B}}_{ij} - \gamma^{\mathrm{B}}_{ij}(x^i_{\mathrm{A}}) = \gamma^{\mathrm{A}}_{ij} + \gamma^{\mathrm{B}}_{ij} - \gamma^{\mathrm{A}}_{ij}(x^i_{\mathrm{B}}) \qquad (1)$$

- Generalised ansatz (1) to unequal-mass binaries by re-defining a conformal factor: Evstafyeva, (2023)

$$\lambda_{\mathrm{new}} = \lambda(x^i) + w_A(x^i)h_A + w_B(x^i)h_B,$$

$h_A, h_b = const.\,, w_A, w_B$ – weight functions

$$\gamma_{ij} = \gamma^{\mathrm{A}}_{ij} + \gamma^{\mathrm{B}}_{ij} - \delta_{ij},$$

$$\lambda = \gamma^{1/3}$$

- Significant progress made on initial data solvers for BS binaries. Siemonsen, (2023)

- Using improved initial data superpositions for equal-mass binaries produces compatible waveforms with initial data obtained from CTS solver, showing a maximum of ~2% difference. Atteneder, (2023)

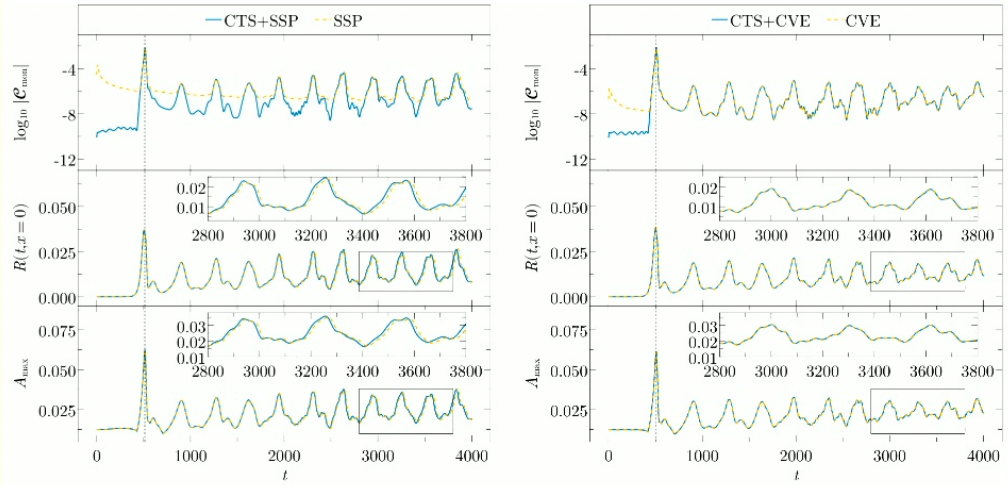

Head-on collisions

$$\varphi(t,r) = A(r)e^{i(\omega t+\delta\phi)}$$

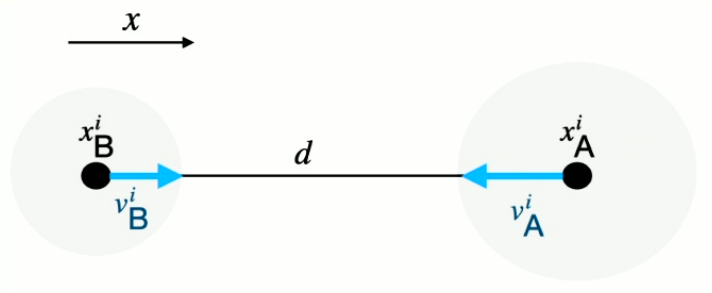

$$\varphi(t,r) = A(r)e^{i\omega t}$$

Energy in head-on collisions

- **For equal-mass collisions**: $\delta\phi = \pi$ is most inefficient in GW emission (thanks to the 'repulsive' nature of the scalar field), whilst $\delta\phi = 0$ is most efficient.
- **For unequal-mass collisions**: the phase difference at merger is no longer the initial dephasing $\delta\phi \Longrightarrow$ horizontal shift in the energy profile is due to the infall-time dependent contribution to the dephasing.
- Smaller mass ratios produce larger GW energy than the equal-mass case: in the BH case, energy is the greatest for the equal-mass binaries, $E \sim \eta^2 = q^2/(1+q)^4$.

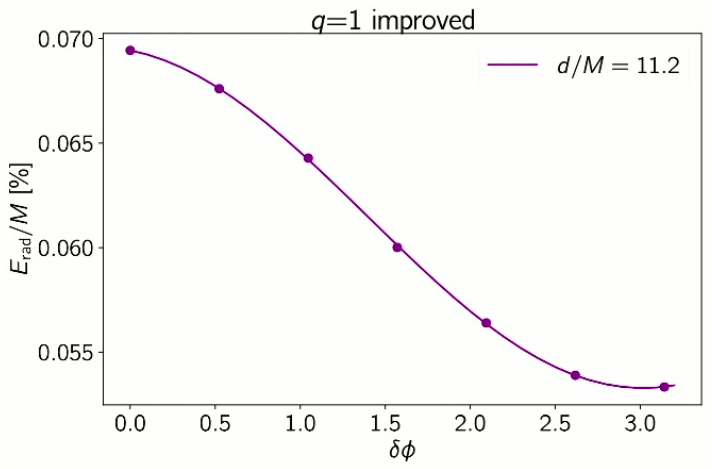

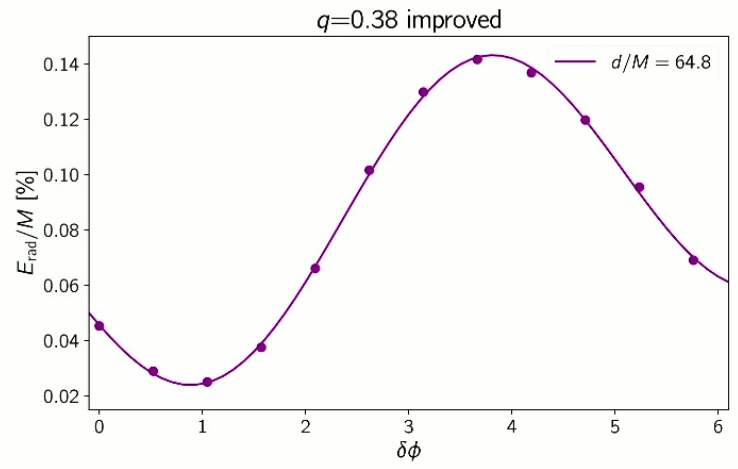

GW signal from unequal-mass head-on collisions

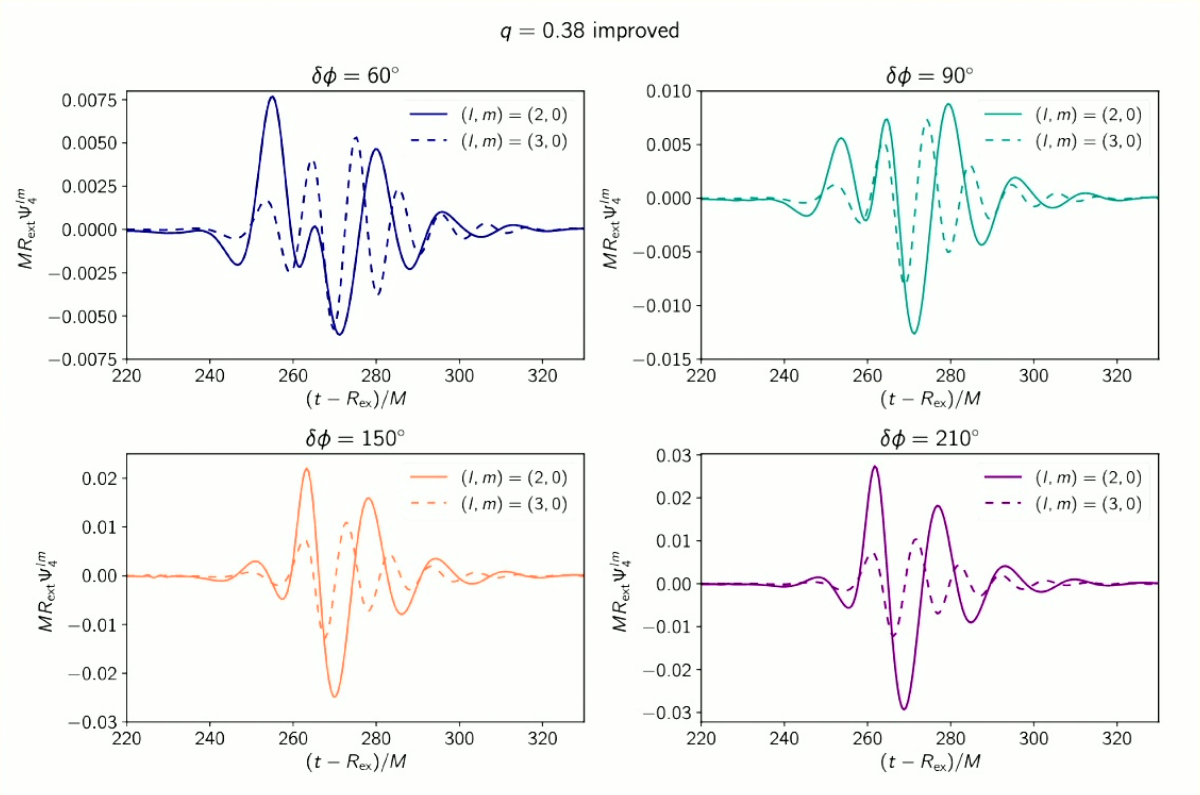

- For $\delta\phi$ resulting in the least GW energy, the signal **exhibits signatures of tidal deformation**.
- Further, in this case the $l = 3$ mode **becomes more comparable** in the amplitude to the $l = 2$ mode.
- This is unlike the head-on BH collision of the same mass ratio, where $l = 3$ mode is roughly 5 times smaller than the $l = 2$ mode.

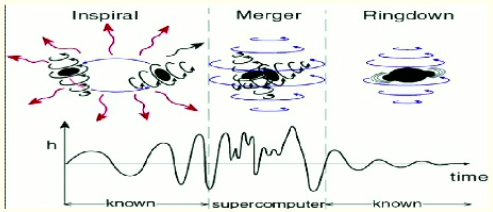

Families of solutions

- By varying $A(0)$, we can construct **families of BS solutions** for a given potential function (e.g. $\sigma_0 = 0.2$). A common feature of $M(R)$ plots is the maximum mass; for a solitonic potential this maximum mass depends on the self-interaction, σ_0.

- We define compactness measure, $C := max(m(r)/r)$.

For comparison:

$C_{NS} \sim 0.1$

$C \approx 0.22$

$C \approx 0.17$

$C \approx 0.12$

$C \approx 0.07$

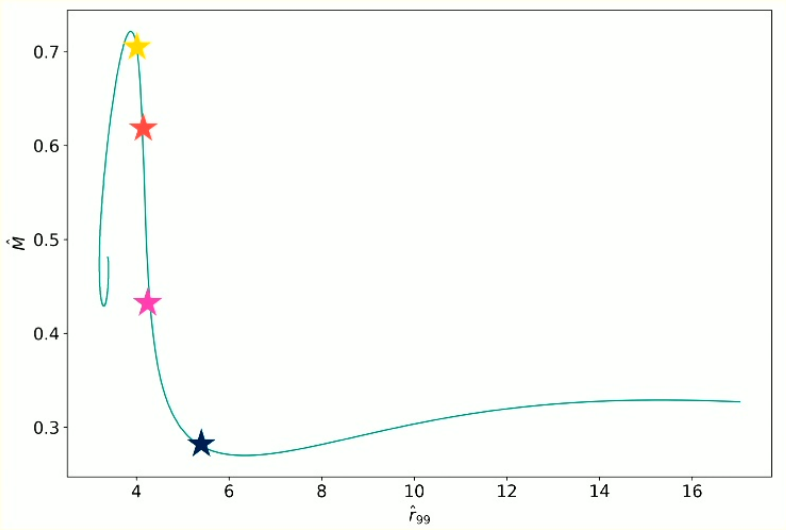

GW signal from unequal-mass head-on collisions

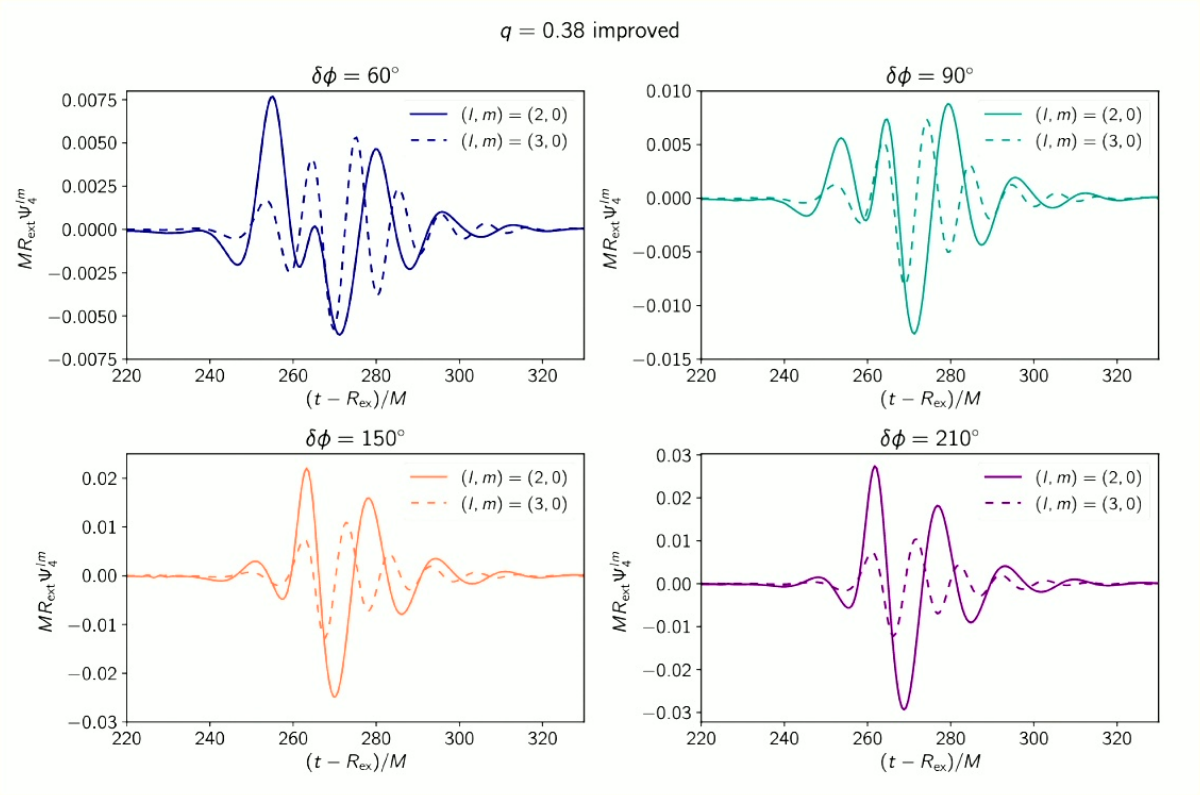

- For $\delta\phi$ resulting in the least GW energy, the signal **exhibits signatures of tidal deformation**.
- Further, in this case the $l = 3$ mode **becomes more comparable** in the amplitude to the $l = 2$ mode.
- This is unlike the head-on BH collision of the same mass ratio, where $l = 3$ mode is roughly 5 times smaller than the $l = 2$ mode.

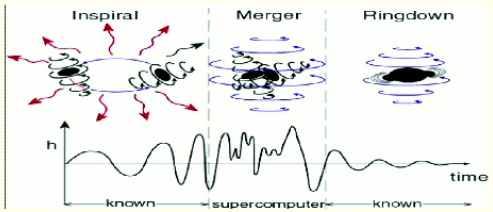

Inspiralling boson star binaries

$$\varphi(t,r) = A(r)e^{i(\omega t+\delta\phi)}$$

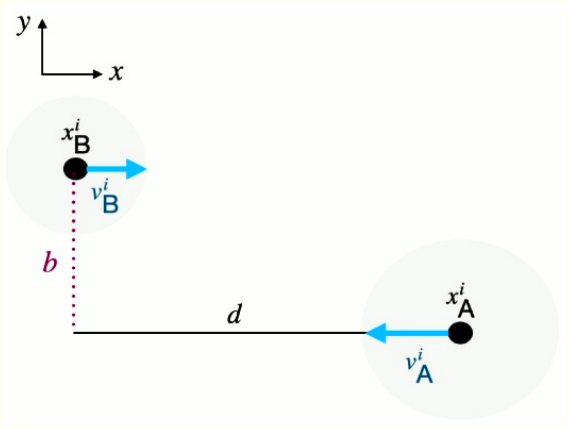

$$\varphi(t,r) = A(r)e^{i\omega t}$$

Recipe to high-precision boson-star inspirals

- 'Appropriate' initial data (e.g. our proposed superposition)– plain superposition results in the two BSs collapsing to BHs in a 1/4 of an orbit!
- Evolution scheme with damping terms (e.g. CCZ4 formulation).
- Appropriate adaptive mesh refinement – poor choices can cause numerical inaccuracies resulting in unphysical features (e.g. departure of the stars).
- Code comparison – GRChombo results compared with Lean code to find excellent agreement.
- Lots of patience!

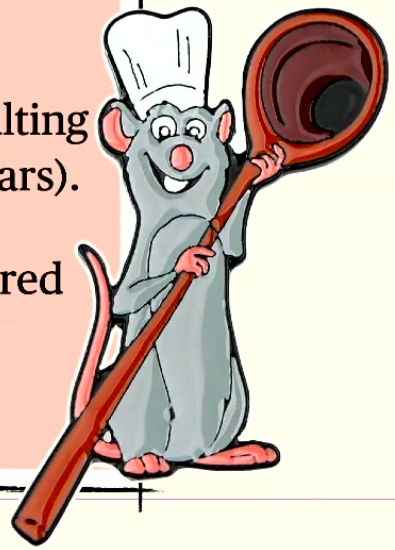

Numerical relativity data set

In what follows next, we will consider **equal-mass, non-spinning** boson star mergers.

Our NR simulations will separate into **two distinct sets**:

Systems containing **compact stars** $C \sim 0.2$.

Systems containing **"fluffy" stars** $C \sim 0.1$.

We will **reduce eccentricity** to low levels of $e \sim 10^{-3}$.

We will focus on binaries completing **15-27 cycles** before merging.

Two main systems: compact stars

- Evolution of equal-mass compact bosons stars results in **BH formation post-merger**.
- Current precision of the BS waveforms is comparable to BH evolutions.

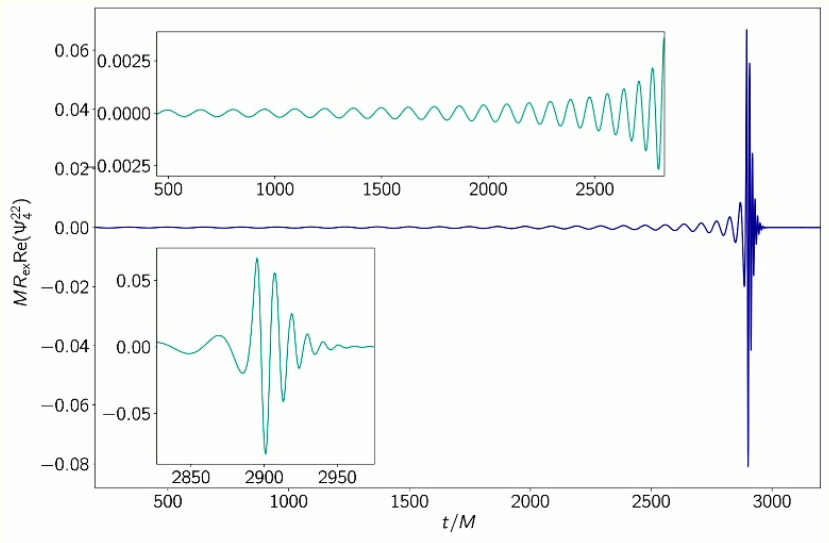

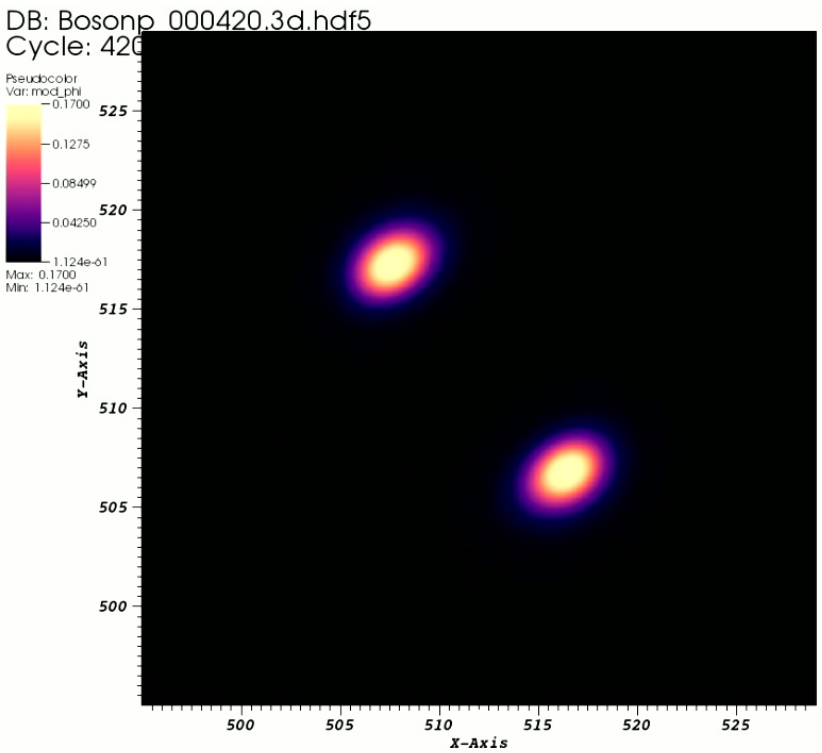

Compact binary stars: possible variations

- **Anti-boson configuration** with one of stars having a rotation in the opposite direction (in the complex plane): $\varphi(t, r) = A(r)e^{-i\omega t}$

- Additional structure is visible pre-merger thanks to scalar interactions. The late inspiral is characterised by larger amplitudes.

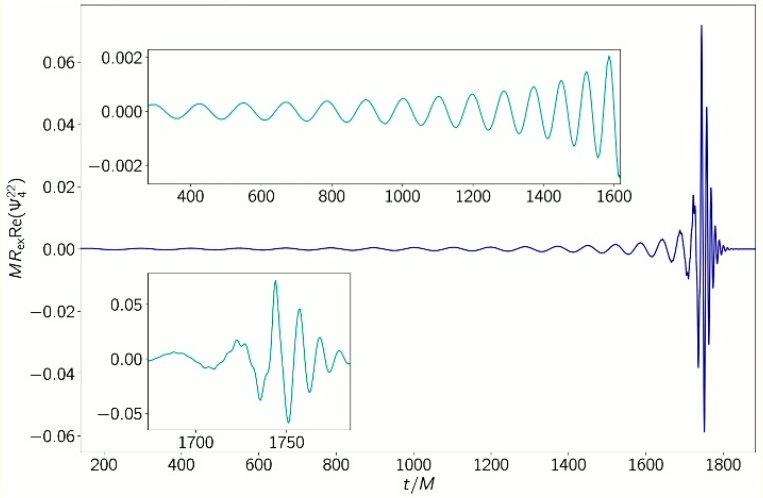

- **Anti-phase configuration** with one of stars having a non-trivial dephasing parameter of $\delta\phi = \pi$.

- The repulsive nature of the scalar field makes the stars more reluctant to merge.

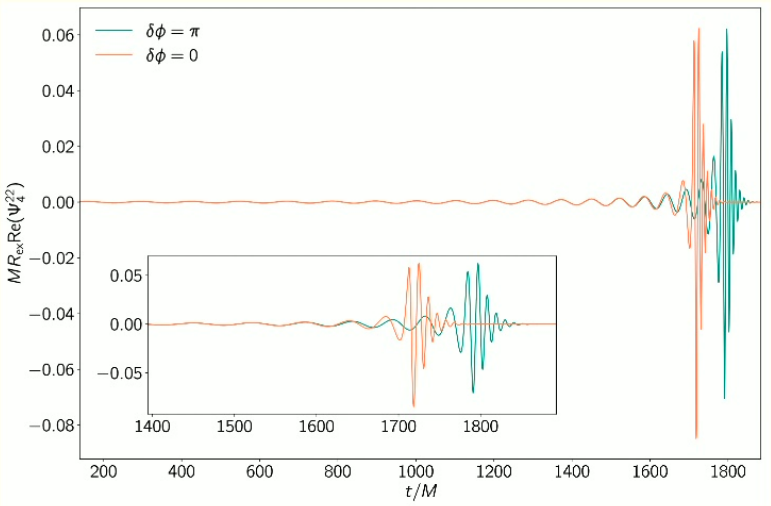

Two main systems: fluffy stars

- Evolution of equal-mass less compact (fluffy) bosons stars results in **BS formation post-merger**.
- The signal is characterised by very faint inspiral and oscillatory ringdown.

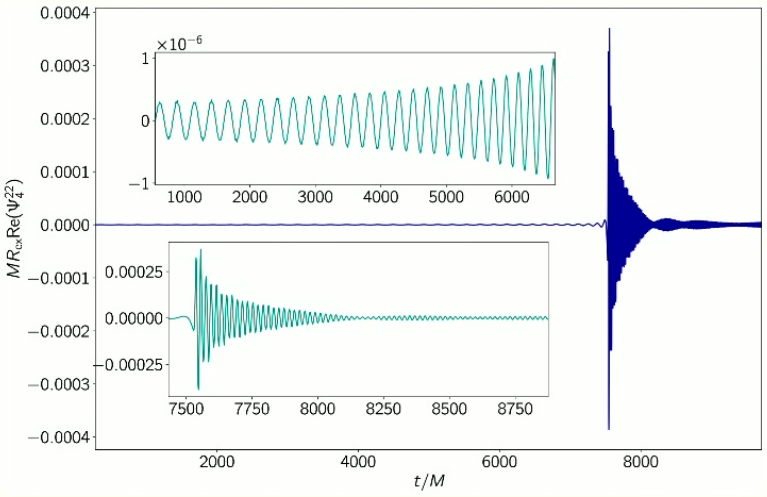

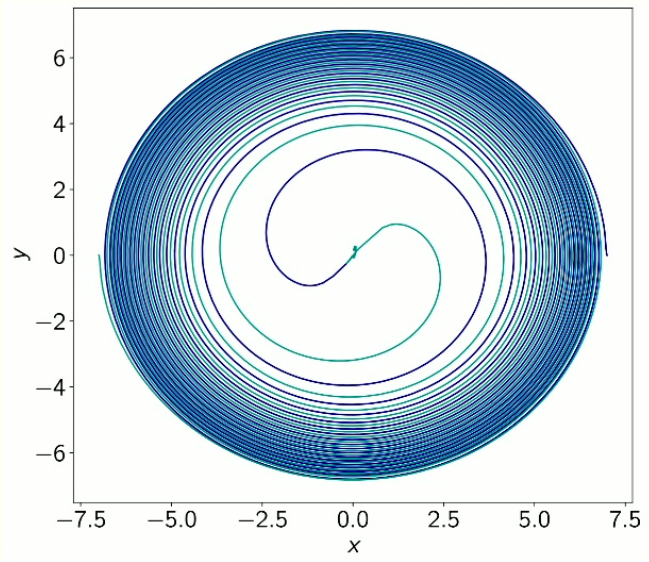

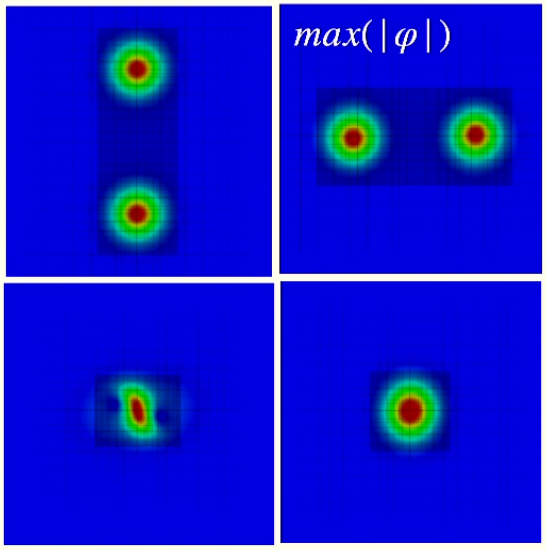

LIGO's response to BS signals

boson star merger

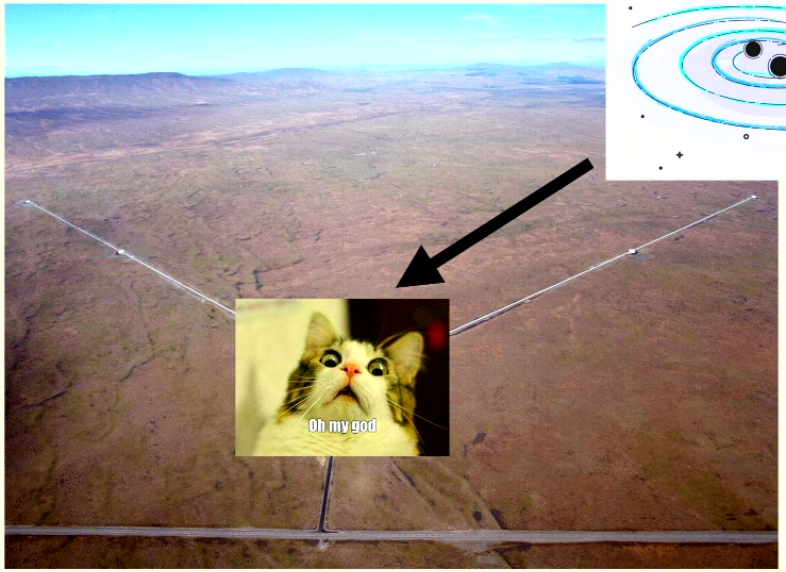

Compact binary stars: possible variations

- **Anti-boson configuration** with one of stars having a rotation in the opposite direction (in the complex plane): $\varphi(t, r) = A(r)e^{-i\omega t}$

- Additional structure is visible pre-merger thanks to scalar interactions. The late inspiral is characterised by larger amplitudes.

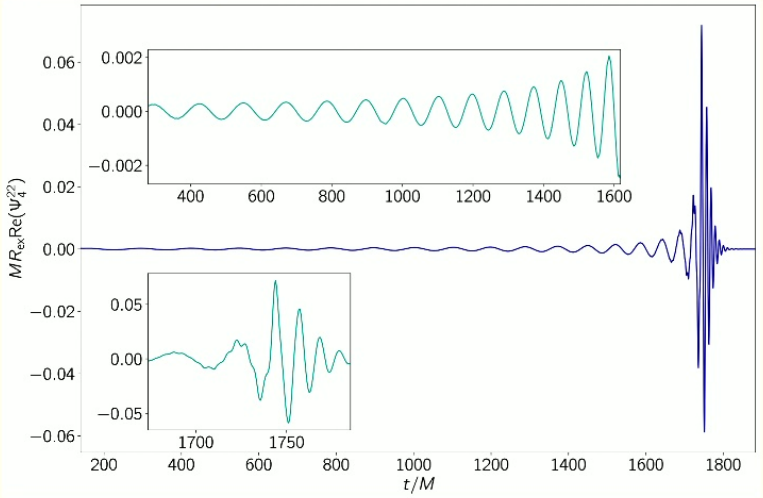

- **Anti-phase configuration** with one of stars having a non-trivial dephasing parameter of $\delta\phi = \pi$.

- The repulsive nature of the scalar field makes the stars more reluctant to merge.

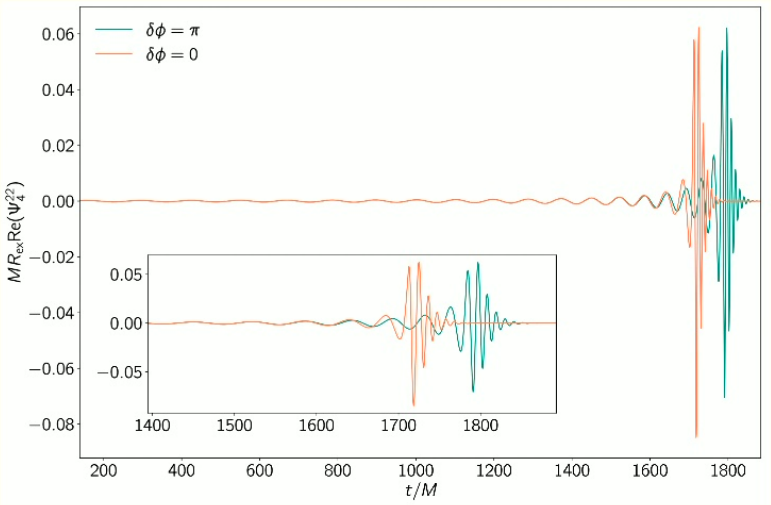

The principles of LIGO analysis

- Large bank of waveform templates/approximants characterised by some **model parameters** θ.

- Say d is **the data associated with a measurement** (NR data or real GW data), *how can we estimate the model parameters for a given event/simulation*? Statistically, this comes down **to constructing a posterior distribution**, $p(\theta|d)$, and using Bayes Theorem:

Likelihood function

Prior

$$p(\theta|d) = \frac{\mathscr{L}(d|\theta)\pi(\theta)}{\mathscr{Z}}, \quad \mathscr{Z} = \int \mathrm{d}\theta \mathscr{L}(d|\theta)\pi(\theta)$$

Evidence

Waveform template

$$L(d;\theta) = \frac{1}{2\pi\sigma^2} \exp\left(-\frac{1}{2}\frac{|d-\mu(\theta)|^2}{\sigma^2}\right)$$

Detector noise

Parameter estimation with Bilby

- **Bilby** is a library for parameter estimation in gravitational-wave astronomy. The main features include: access to multiple sampling algorithms (e.g. nested samplers), a range of LIGO waveform approximants, freedom to customise waveform models and likelihood functions.

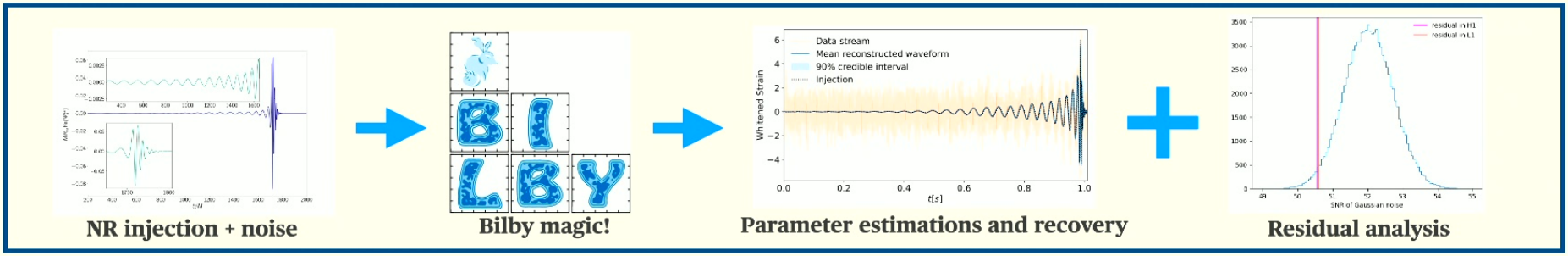

- In order to assess the quality of the waveform approximant in capturing the injection, we perform **residual analysis**. Define **residual** as $r := s - h_{max}$, where s is the signal perceived by the detector and h_{max} is the waveform approximant maximising the log-likelihood.

- For a given length of detector data, we can construct a distribution of optimal SNR for Gaussian noise. If the waveform approximant captured the NR injection well, the optimal SNR of the residual must fall within the support of such distribution.

Waveform approximants

- Ample amount of approximants to choose from:

e.g. *IMRPhenomD, IMRPhenomXP, IMRPhenomXPHM, IMRPhenomPv3* for **BH binaries**

TaylorF2, IMRPhenomPv2_NRTidalv2 waveforms modelling for **NS binaries inspirals only**.

TABLE I. Default binary black hole priors. The intrinsic variables are the two black hole masses $m_{1,2}$, their dimensionless spin magnitudes $a_{1,2}$, the tilt angle between their spins and the orbital angular momentum $\theta_{1,2}$, and the two spin vectors describing the azimuthal angle separating the spin vectors $\delta\phi$ and the cone of precession about the system's angular momentum $\phi_{\rm JL}$. The extrinsic parameters are the luminosity distance d_L, the right ascension ra and declination dec, the inclination angle between the observers line of sight and the orbital angular momentum ι, the polarisation angle ψ, and the phase at coalescence ϕ_c. The phase, spins, and inclination angles are all defined at some reference frequency. We do not set a default prior for the coalescence time t_c. 'sin' and 'cos' priors are uniform in cosine and sine, respectively, and 'comoving' implies uniform in comoving volume.

variable	unit	prior	minimum	maximum
$m_{1,2}$	$M_\odot$	uniform	5	100
$a_{1,2}$	-	uniform	0	0.8
$\theta_{1,2}$	rad.	sin	0	π
$\delta\phi$, $\phi_{\rm JL}$	rad.	uniform	0	2π
d_L	Mpc	comoving	10^2	5×10^3
ra	rad.	uniform	0	2π
dec	rad.	cos	$-\pi/2$	$\pi/2$
ι	rad.	sin	0	π
ψ	rad.	uniform	0	π
ϕ_c	rad.	uniform	0	2π

Ashton, (2019)

Waveform Family	Domain	Waveform Model	Spins		Mode Content	Eccentricity	Calibration Region
1st generation	FD	IMRPhenomA	✕		(2,±2)	no	q ≤ 4
2nd generation	FD	IMRPhenomB	✓		(2,±2)	no	NR calibration: q ≤ 4, $\chi_{1/2}$ ≤ 0.75, $\chi_{1/2}$ ≤ 0.85 (for q = 1)
2nd generation	FD	IMRPhenomC	✓		(2,±2)	no	NR calibration: q ≤ 4, $\chi_{1/2}$ ≤ 0.75, $\chi_{1/2}$ ≤ 0.85 (for q = 1)
2nd generation	FD	IMRPhenomP	✓✓	CP	(2,±2)	no	NR calibration: q ≤ 4, $\chi_{1/2}$ ≤ 0.75, $\chi_{1/2}$ ≤ 0.85 (for q = 1)
3rd generation	FD	IMRPhenomD	✓		(2,±2)	no	NR calibration: q ≤ 18, $\lvert\chi_{1/2}\rvert$ ≤ 0.85, -0.95 ≤ $\chi_{1/2}$ ≤ 0.98 (for q = 1)
3rd generation	FD	IMRPhenomPv2	✓✓	CP	(2,±2)	no	NR calibration: q ≤ 18, $\lvert\chi_{1/2}\rvert$ ≤ 0.85, -0.95 ≤ $\chi_{1/2}$ ≤ 0.98 (for q = 1)
3rd generation	FD	IMRPhenomPv3	✓✓	CP	(2,±2)	no	NR calibration: q ≤ 18, $\lvert\chi_{1/2}\rvert$ ≤ 0.85, -0.95 ≤ $\chi_{1/2}$ ≤ 0.98 (for q = 1)
3rd generation	FD	IMRPhenomHM	✓		(2,±2),(2,±1),(3,±3),(4,±3),(4,±4)	no	NR calibration: q ≤ 18, $\lvert\chi_{1/2}\rvert$ ≤ 0.85, -0.95 ≤ $\chi_{1/2}$ ≤ 0.98 (for q = 1)
3rd generation	FD	IMRPhenomPv3HM	✓✓	CP	(2,±2),(2,±1),(3,±3),(4,±3),(4,±4)	no	NR calibration: q ≤ 18, $\lvert\chi_{1/2}\rvert$ ≤ 0.85, -0.95 ≤ $\chi_{1/2}$ ≤ 0.98 (for q = 1)
4th generation	FD	IMRPhenomXAS	✓		(2,±2)	in development	NR calibration: q ≤ 18, $\chi_{1/2}$ ≤ 0.99 Teukolsky calibration: q ≤ 1000
4th generation	FD	IMRPhenomXP	✓✓	CP	(2,±2)	in development	NR calibration: q ≤ 18, $\chi_{1/2}$ ≤ 0.99 Teukolsky calibration: q ≤ 1000
4th generation	FD	IMRPhenomXHM	✓		(2,±2),(2,±1),(3,±2),(3,±3),(4,±4)	in development	NR calibration: q ≤ 18, $\chi_{1/2}$ ≤ 0.99 Teukolsky calibration: q ≤ 1000
4th generation	FD	IMRPhenomXPHM	✓✓	CP	(2,±2),(2,±1),(3,±2),(3,±3),(4,±4)	in development	NR calibration: q ≤ 18, $\chi_{1/2}$ ≤ 0.99 Teukolsky calibration: q ≤ 1000
4th generation	TD	IMRPhenomT	✓		(2,±2)	in development	NR calibration: q ≤ 18, $\chi_{1/2}$ ≤ 0.99 Teukolsky calibration: q ≤ 1000
4th generation	TD	IMRPhenomTP	✓✓	CP	(2,±2)	in development	NR calibration: q ≤ 18, $\chi_{1/2}$ ≤ 0.99 Teukolsky calibration: q ≤ 1000
4th generation	TD	IMRPhenomTHM	✓		(2,±2),(2,±1),(3,±3),(4,±4),(5,±5)	in development	NR calibration: q ≤ 18, $\chi_{1/2}$ ≤ 0.99 Teukolsky calibration: q ≤ 1000
4th generation	TD	IMRPhenomTPHM	✓✓	CP	(2,±2),(2,±1),(3,±3),(4,±4),(5,±5)	in development	NR calibration: q ≤ 18, $\chi_{1/2}$ ≤ 0.99 Teukolsky calibration: q ≤ 1000

✕ no spins ✓ spins aligned with orbital angular momentum ✓✓ precessing spins CP mode content in co-precessing frame

LISA Consortium Waveform Working Group, (2023)

Results: compact binaries of $M_{tot} > 40M_{\odot}$

- BH waveforms approximants are able to recover the injected signals very well for binaries of total masses $M_{tot} > 40M_{\odot}$ and performing a residual analysis confirms that the residual r is compatible with Gaussian noise. **However, the approximants fail to recover the injected parameters**. The injected parameters, such as mass, spins do not even lie within the support of posterior distributions.

- The 'best' recovery of injected parameters is achieved for the anti-boson configuration.

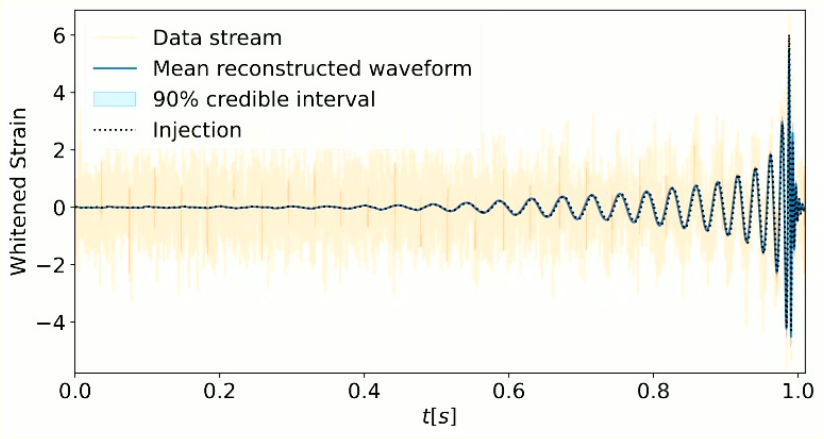

Recovery of equal-mass non-spinning BS binary of total mass $80M_{\odot}$ with IMRPhenomXP template.

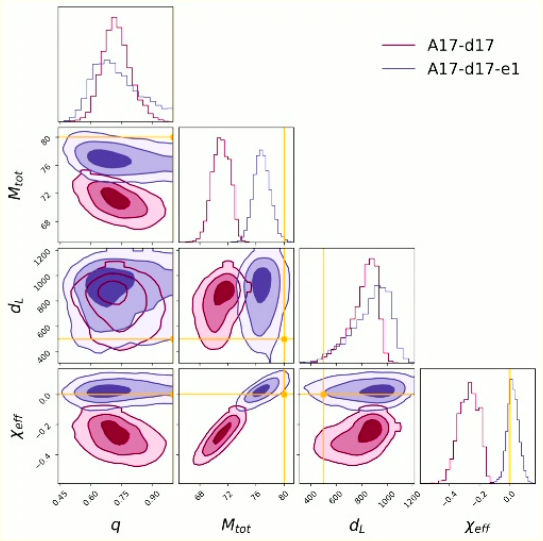

Comparison of parameter estimation for equal-mass BS injection (pink contours) and equal-mass anti-boson injection (purple contours).

Results: compact binaries of $M_{tot} \leq 40M_{\odot}$

- For smaller total masses, the inspiral amplitude becomes more significant compared to the rest of the signal => additional information makes it harder for the BH waveforms to recover the injected BS signals!

- BH waveform templates fail to recover the signal, leaving a **non-Gaussian residual**.

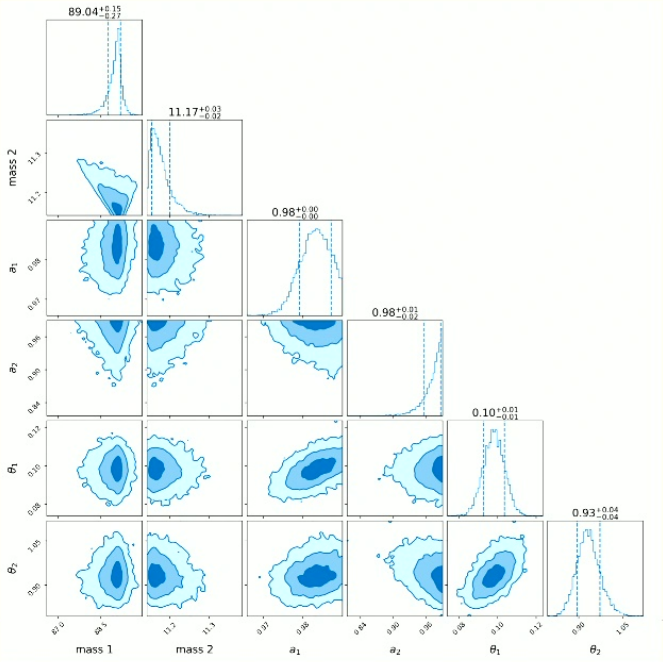

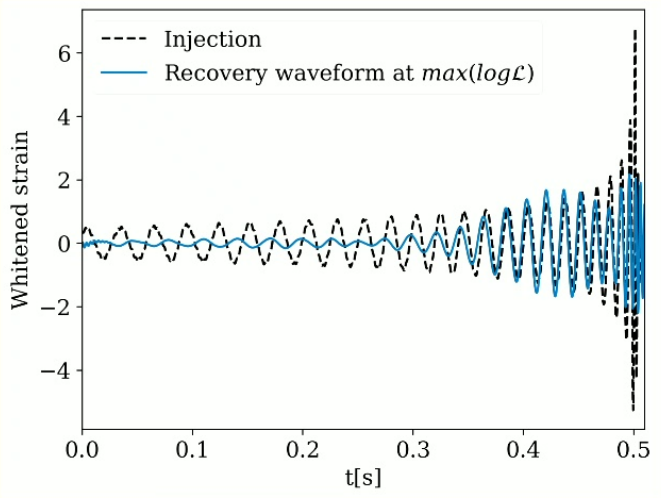

Recovery of equal-mass non-spinning BS binary of total mass $40M_{\odot}$ with IMRPhenomXP approximant.

Results: fluffy binaries

- **NS inspiral-only waveform approximants model the inspiral part of the injected BS waveform fairly well**, leaving a Gaussian residual.
- The parameter estimation still lacks agreement with the injected parameters.

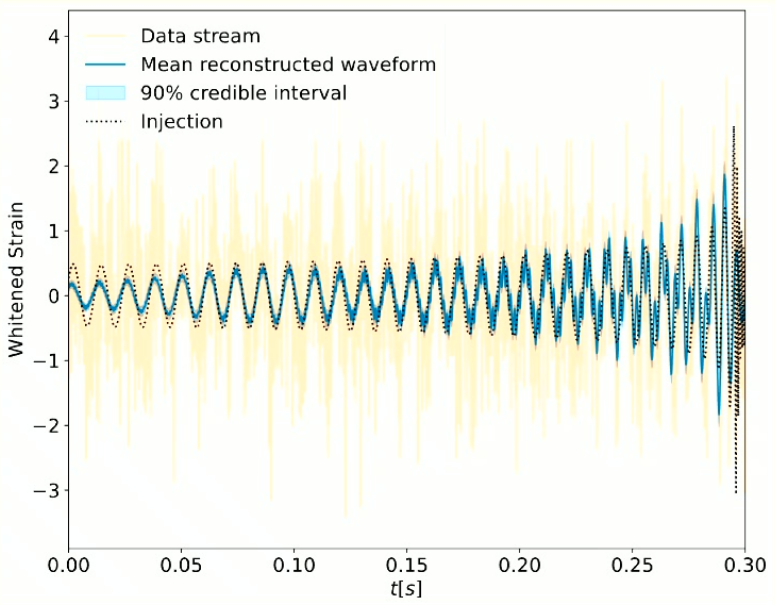

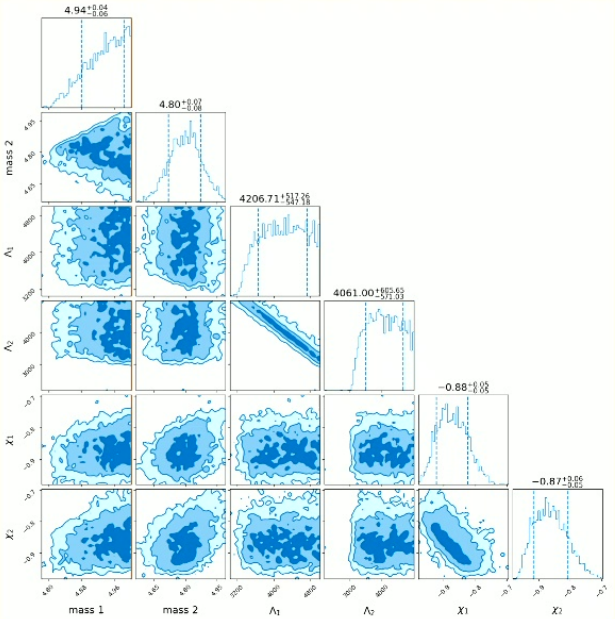

Recovery of equal-mass non-spinning BS binary of total mass $10M_\odot$ with TaylorF2 approximant.

Expected tidal deformability $\Lambda \sim 1000$.

Conclusions and outlook

1. Initial data construction is crucial for mitigating the spurious features of plainly superposed initial data for binaries of arbitrary mass ratio.

2. Inspiralling configurations of less compact stars forming a BS post-merger and/or head-on unequal-mass collisions, resulting in least GW energy, present a clear example of the diversity of the parameter space for BSs, with distinct features from a BH case.

3. High precision NR simulations of boson stars mergers is possible, however a lot of the parameter space is yet to be explored.

There is more to do!

- **Implementation of initial data solver routine.**
- **Further exploration of the parameter space.**
- **Ringdown analysis.**
- **3+1 BS evolutions in scalar-tensor theory.**

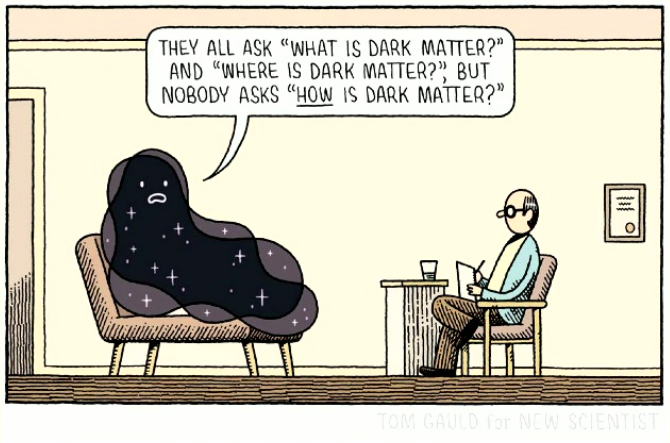

Thank you!